Nine-channel wavelength tunable single mode laser array based on slots

Wei-Hua Guo,[1,*] Qiaoyin Lu,[2] Marta Nawrocka,[2] Azat Abdullaev,[2] James O'Callaghan,[3] and John F. Donegan[2]

[1]*Department of Electrical & Computer Engineering, University of California Santa Barbara, CA 93106, USA*
[2]*School of Physics, Trinity College Dublin, Dublin 2, Ireland*
[3]*Tyndall National Institute, University College Cork, Ireland*
[*]*guow@ece.ucsb.edu*

Abstract: A 9-channel wavelength tunable single-mode laser array based on slots is presented. The fabricated laser array demonstrated a threshold current in a range of 19~21 mA with the SOA unbiased at 20°C under continuous wave condition. Stable single mode performances have been observed with side-mode suppression-ratio (SMSR) > 50 dB. The output power higher than 37 mW was obtained at the SOA injected current of 70 mA for all the 9 channels within the laser array. A wavelength quasi-continuous tuning range of about 27 nm has been achieved for the laser array with the temperature variations from 10°C to 45°C. This array platform is of a single growth and monolithically integrable. It can be easily fabricated by standard photolithography. In addition, it potentially removes the yield problem due to the uncertainty of the facet cleaving.

OCIS codes: (250.0250) Optoelectronics; (250.5960) Semiconductor lasers; (140.3570) Lasers, single-mode; (250.5300) Photonic integrated circuits.

References and links

1. J. De Merlier, K. Mizutani, S. Sudo, K. Naniwae, Y. Furushima, S. Sato, K. Sato, and K. Kudo, "Full C-band external cavity wavelength tunable laser using a liquid-crystal-based tunable mirror," IEEE Photon. Technol. Lett. **17**(3), 681–683 (2005).
2. L. A. Coldren, G. A. Fish, Y. Akulova, J. S. Barton, L. Johansson, and C. W. Coldren, "Tunable semiconductor lasers: a tutorial," J. Lightwave Technol. **22**(1), 193–202 (2004).
3. Y. Tohmori, Y. Yoshikuni, H. Ishii, F. Kano, T. Tamamura, Y. Kondo, and M. Yamamoto, "Broad-range wavelength-tunable superstructure grating (SSG) DBR lasers," IEEE J. Quantum Electron. **29**(6), 1817–1823 (1993).
4. A. J. Ward, D. J. Robbins, G. Busico, E. Barton, L. Ponnampalam, J. P. Duck, N. D. Whitbread, P. J. Williams, D. C. J. Reid, A. C. Carter, and M. J. Wale, "Widely tunable DS-DBR laser with monolithically integrated SOA: Design and performance," IEEE J. Sel. Top. Quantum Electron. **11**(1), 149–156 (2005).
5. D. C. Byrne, J. P. Engelstaedter, W. H. Guo, Q. Y. Lu, B. Corbett, B. Roycroft, J. O'Callaghan, F. H. Peters, and J. F. Donegan, "Discretely tunable semiconductor lasers suitable for photonic integration," IEEE J. Sel. Top. Quantum Electron. **15**(3), 482–487 (2009).
6. T. Yu, L. Zou, L. Wang, and J.-J. He, "Single-mode and wavelength tunable lasers based on deep-submicron slots fabricated by standard UV-lithography," Opt. Express **20**(15), 16291–16299 (2012).
7. H. Ishii, K. Kasaya, and H. Oohashi, "Narrow spectral linewidth operation (<160kHz) in widely tunable distributed feedback laser array," Electron. Lett. **46**(10), 714–715 (2010).
8. B. Kelly, R. Phelan, D. Jones, C. Herbert, J. O'Carroll, M. Rensing, J. Wendelboe, C. B. Watts, A. Kaszubowska-Anandarajah, P. Perry, C. Guignard, L. P. Barry, and J. O'Gorman, "Discrete mode laser diodes with very narrow linewidth emission," Electron. Lett. **43**(23), 1282–1283 (2007).
9. J. P. Engelstaedter, B. Roycroft, and B. Corbett, "Laser and detector using integrated reflector for photonic integration," Electron. Lett. **44**(17), 1017–1019 (2008).
10. S. O'Brien, F. Smyth, Kai Shi, J. O'Carroll, P. M. Anandarajah, D. Bitauld, S. Osborne, R. Phelan, B. Kelly, J. O'Gorman, F. H. Peters, B. Roycroft, B. Corbett, and L. P. Barry, "Design, characterization, and applications of index-patterned Fabry-Perot Lasers," IEEE J. Sel. Top. Quantum Electron. **17**(6), 1621–1631 (2011).
11. Y. Li, Y. Xi, X. Li, and W.-P. Huang, "Design and analysis of single mode Fabry-Perot lasers with high speed modulation capability," Opt. Express **19**(13), 12131–12140 (2011).

#186129 - $15.00 USD Received 28 Feb 2013; revised 12 Apr 2013; accepted 12 Apr 2013; published 17 Apr 2013

12. Y. Wang, Y. Yang, S. Zhang, L. Wang, and J.-J. Hou, "Narrow linewidth single-mode slotted Fabry-Perot laser using deep etched trenches," IEEE Photon. Technol. Lett. **24**(14), 1233–1235 (2012).
13. Q. Lu, W.-H. Guo, D. Byrne, and J. F. Donegan, "Design of slotted single mode lasers suitable for photonic integration," IEEE Photon. Technol. Lett. **22**(11), 787–789 (2010).
14. W.-H. Guo, Q. Lu, M. Nawrocka, A. Abdullaev, M. Lynch, V. Weldon, and J. F. Donegan, "Integrable slotted single mode lasers," IEEE Photon. Technol. Lett. **24**(8), 634–636 (2012).
15. Q. Lu, W.-H. Guo, M. Nawrocka, A. Abdullaev, C. Daunt, J. O'Callaghan, M. Lynch, V. Weldon, F. Peters, and J. F. Donegan, "Single mode lasers based on slots suitable for photonic integration," Opt. Express **19**(26), B140–B145 (2011).
16. Q. Lu, W.-H. Guo, A. Abdullaev, M. Nawrocka, M. Lynch, V. Weldon, and J. F. Donegan, "Two-section single mode lasers based on slots suitable for photonic integration," Electron. Lett. **48**(15), 945–946 (2012).
17. Q. Lu, A. Abdullaev, M. Nawrocka, W.-H. Guo, and J. F. Donegan, "Single mode lasers based on slots integrated with a semiconductor optical amplifier," IEEE Photon. Technol. Lett. **25**, 564–567 (2013).
18. W.-H. Guo, D. C. Byrne, Q. Lu, B. Corbett, and J. F. Donegan, "Fabry-Perot laser characterization based on the amplified spontaneous emission spectrum and the Fourier series expansion method," IEEE J. Sel. Top. Quantum Electron. **17**(5), 1356–1363 (2011).

1. Introduction

Wavelength-tunable semiconductor lasers are key components for the future dense-wavelength division-multiplexed (DWDM) optical communication system. So far, a number of wavelength-tunable lasers have been developed such as external cavity lasers [1], sampled-grating distributed Bragg reflector (SG-DBR) lasers [2], super-structure grating distributed Bragg reflector (SSG-DBR) lasers [3], digital supermode distributed.

Bragg reflector (DS-DBR) lasers [4]. Tunable lasers based on surface gratings have also been demonstrated, which has the cost advantages due to its simple process [5,6] compared with the conventional buried DBR based lasers.

Single mode laser arrays are another option to produce a tunable laser, where a set of individual single mode lasers are monolithically fabricated on one chip and each one can be tuned over a limited range (normally ~5 nm). Compared with other types of tunable lasers, these kinds of lasers have advantages of stable laser performance without mode-hops. Recently, such a laser array based on buried DFB gratings has been reported with a narrow linewidth of 160 kHz over 40 nm tuning range [7], which makes it much more suitable for coherent communications systems. However, fabricating such laser arrays requires both high resolution processing and complex re-growth steps.

Realizing lasers with very simple fabrications has attracted a lot of interests over the world [8–12]. Recently, by introducing a group of slots into the surface of the ridge on one side of the laser cavity, we have successfully designed and demonstrated single mode lasers with side mode suppression ratio (SMSR) more than 50 dB [13,14]. Such a laser has also been demonstrated to integrate with an EA modulator using identical active layer (IAL) [15]. This laser structure is monolithically integrable, regrowth free and can be fabricated using standard photolithography. Therefore such a laser platform has several advantages that firstly it has a significant cost reduction, secondly it enables the use of AlGaInAs material for un-cooled operation, and lastly it enables the integration with semiconductor optical amplifiers (SOA) to control the output power. To potentially solve the single mode yield problem due to the uncertainty of the cleaved facet position, we further presented the two-section slotted single mode laser structure [16]. By integrating a monolithic SOA, the laser has demonstrated an output power more than 45 mW [17].

In this work, we present a 9-channel single mode laser array based on such laser platform. Results show that the fabricated laser array spans a discrete wavelength range from 1540 to 1563 nm with the side-mode suppression-ratio more than 50 dB for all the 9 channels within the array.

2. Device structure

The schematic structure of the slotted single mode laser array is shown in Fig. 1(a). Each laser of the array has a typical 2.0 μm-wide surface ridge waveguide structure. The laser epitaxial

#186129 - $15.00 USD Received 28 Feb 2013; revised 12 Apr 2013; accepted 12 Apr 2013; published 17 Apr 2013

structure is based on a standard 1550 nm LD design. The active region consists of five AlGaInAs quantum wells. Above it are 1.6 μm-thick p-doped InP layer, 50 nm-thick p-doped InGaAsP layer, and 200 nm-thick InGaAs contact layer. One side of each laser has multiple uniformly distributed slots which act as an active DBR reflector of the laser and provide sufficient one side (front) feedback for lasing operation. The other (back) side reflection is provided by the facet. Because in this case we still need to cleave the back facet, there is a single mode issue caused by the uncertainty of this cleaving position. To remove this yield problem, each laser is divided into two sections electrically isolated by the last slot from the group of slots as seen from Fig. 1 (a): the front section includes a group of slots and the back section consists of straight waveguide section. By tuning the back section current of some lasers in the array, i.e., tuning the longitudinal mode position relative to the reflection peak, it is possible to make a laser array with good single mode performance for all the channels. Considering the loss caused by the etched slots, a SOA is naturally integrated with but electrically isolated from each laser to boost the output power. To reduce the reflection from the front facet, the SOA section is curved to generate a 7° angle from the normal of the facet. To further improve the laser performance in terms of increasing the output power and reducing the threshold current, the antireflection (AR) and high reflection (HR) coating films are applied to the front and the back facets of the laser array, respectively.

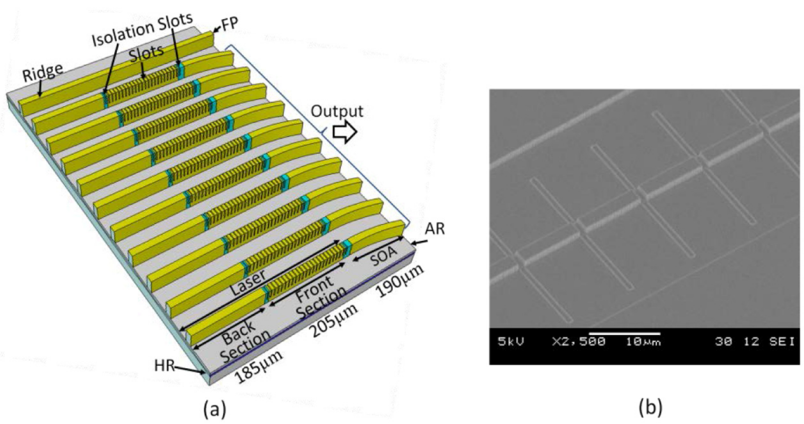

Fig. 1. (a) 3D schematic structure of tunable slotted single mode laser array. (b) SEM picture of etched slots.

For each laser in the array, the slot parameters such as slot width, depth, and number are key parameters which need to be optimized. The 2D scattering matrix method was used for the optimization. For ease of fabrication, the slot width is optimized to be around 1.1 μm wide, which makes the laser compatible with standard photolithography. The slot depth was optimized to be 1.35 μm which is much less than the 1.85 μm ridge height. For such a slot depth a single slot can provide around 1% and 97% amplitude reflection and transmission, respectively. Because the reflection from a single slot is quite weak, a group of slots are used to provide sufficient feedback for the lasing operation. The slot period is optimized to be around 9 μm to obtain a high reflection from the slots, which means the slots act as a high order surface grating with 37th grating order. For the trade-off between maximizing the reflectivity while minimizing the bandwidth of the reflection peaks and keeping the cavity length short, the slot number are optimized to be 24, which generate an amplitude reflection and transmission of around 0.43 and 0.4, respectively. Such a group of slots ensure that the reflection spectrum has a narrow bandwidth to achieve a good single mode operation with minimum threshold. The laser array is designed to have a frequency spacing of 400 GHz (3.2 nm) which is obtained by slight changing the slot period according to:

#186129 - $15.00 USD Received 28 Feb 2013; revised 12 Apr 2013; accepted 12 Apr 2013; published 17 Apr 2013

$$d_p = \frac{m\lambda_B}{2n_{eff}}. \tag{1}$$

where the d_p is the slot period, λ_B is the Bragg wavelength, n_{eff} is the average effective refractive index in waveguide structure and m is grating order which is 37. For all of the 9-channel lasers in the array, lasing wavelengths are designed as 1542.2, 1545.4, 1548.6, 1551.8, 1555, 1558.2, 1561.4, 1564.6, and 1567.8 nm with a channel spacing of 3.2 nm.

3. Device fabrication and characteristics

The designed laser array was fabricated using the similar process in [16]. Two steps of inductively coupled plasma (ICP) based dry etching with Cl_2 /N_2 gas combinations were used to form the ridge and the slots. The ridge was etched with a height of 1.8 μm which resulted in a slot depth of about 1.3 μm with 0.5 μm shallower than the ridge as was determined by this two-step dry etching process. The four corners of etched slots are quite sharp, as shown in Fig. 1(b) of the SEM pictures of the etched slots. But there are also issues with the fabrication as seen from the SEM picture: there are residual InP walls left beside the ridge at the slot positions which we think have increased the loss of slots. The total length of each laser in the fabricated array is around 400 μm integrated with the 190 μm long curved front SOA. The back section of the laser was about 185 μm long between the back facet and the first slot (from left). The front section was about 205 μm long slot section. After the ridge was passivated and metal contacted (the electrode metal covered the slots area except for the isolation slots), the laser array bars were coated with high reflection and antireflection films. Finally, the laser arrays were cleaved into individual bars mounted on AlN carriers.

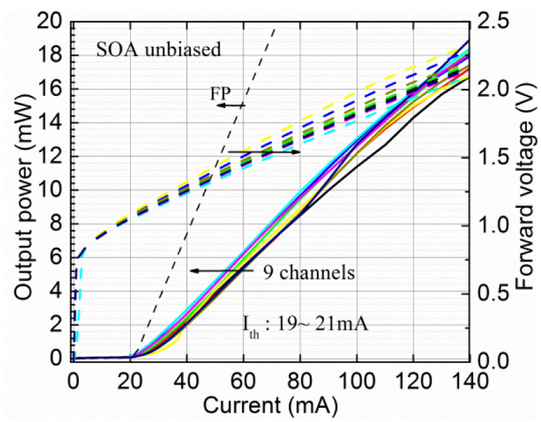

Fig. 2. Measured light-current-voltage (L-I-V) curve for all the 9-channel laser array and the FP laser on same chip at 20°C under CW condition.

The mounted device was placed on a copper heat sink which was mounted on a thermoelectric cooler (TEC) to control the chip temperature. The laser array was test at 20°C under continuous-wave (CW) condition and to remove the FP cavity influence, the SOA was left unbiased. First we electrically connected the front section and back section of each laser together and measured the light-current-voltage curves of these lasers. Figure 2 shows the typical LIV curves for all of the 9 channels within the array. The HR coated back facet produce a high reflection which results in a low threshold current of about 19~21 mA. In this case, because some lasers such as the channels 1, 7 and 8 have unsuitable cleaving positions of the back facets, the longitudinal modes do not coincide well with the reflection peak for these channel lasers, thus results in mode hopping between the neighbored longitudinal modes as shown by the kinks from the LI curves. For comparison, a FP laser fabricated on the same chip was also measured as shown in Fig. 2. It is found that the slope efficiency of the slotted

#186129 - $15.00 USD Received 28 Feb 2013; revised 12 Apr 2013; accepted 12 Apr 2013; published 17 Apr 2013

laser is reduced to around half of the FP laser due to the loss caused by the etched slots. By measuring the amplified spontaneous emission (ASE) spectra of FP lasers fabricated with the same process, we calculated the net modal gain spectrum using Fourier series expansion method [18]. For the current density of 2.3 kA/cm^2 (threshold ~19 mA), the corresponding net mode gain estimated is around 35 cm^{-1}. Thus the amplitude reflection $|r|$ and transmission $|t|$ from 24 slots are calculated as 0.54 and 0.62, respectively, using the scattering matrix method. This yields a loss ($1-|r|^2-|t|^2$) about 0.3. The imperfect slot fabrication and the unbiased SOA reduce the slope efficiency further. All of these factors together roughly explain the slope efficiency drop of the single mode laser compared with the FP laser on the same bar.

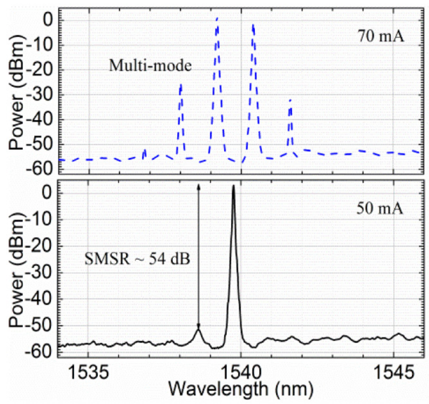

Fig. 3. Measured output spectrum vs. back section current for the channel 1 laser.

The output light from the laser array was collected by a lensed single mode fiber and analyzed by an Agilent 86140B optical spectrum analyzer (OSA). The resolution of the OSA was set to be 0.06 nm with sensitivity of −80 dBm. For the channel laser number 1, 7 and 8, because the longitudinal modes do not coincide well with the reflection peak due to the unsuitable back facet cleaving position, the front and back sections of these lasers were separately biased. To achieve a good single mode performance, the current of the back section was adjusted slightly (keeping the front section current constant) to tune the longitudinal mode position in order to align with the reflection peak. Figure 3 shows typically how such laser tuning behavior varied with different back section current for the channel 1 laser at 15°C. It was found that the SMSR reached 54 dB when the injected back current was 50 mA for this channel.

Figure 4(a) shows the recorded spectra for all 9 channel lasers at the total current of around 130 mA with the SOA section unbiased, where, for the channels 1, 7 and 8, the front section current was kept constant as 65 mA while the back section current was adjusted to 45, 55, 75 mA, respectively, to achieve a good single mode performance [16]. Stable single mode performances were observed with side-mode suppression-ratio (SMSR) more than 50 dB for all the 9-channel lasers. The lasing wavelengths were around 1540.02nm, 1542.69nm, 1545.76nm, 1548.95nm, 1551.93nm, 1555.18nm, 1558.04nm, 1560.43 and 1563.11 which had a slight blue shift of around 3 nm from the design. The channel spacings among all the 9 channels are within the range from 2.39 nm to 3.25 nm different from the design due to the back current tuning. Considering a tuning slope of about 0.1 nm/degree, a temperature change of about 32.5 ˚C is needed to make a wavelength tuning of 3.25 nm (400 GHz) to cover the channel spacing. That means in this case the laser array can work over a wide wavelength range continuously. The output power of the laser array was measured by keeping the above currents set-up for each channel laser. Figure 4(b) shows the measured output power as a function of the SOA injection current. The output power was more than 37 mW at a current

#186129 - $15.00 USD Received 28 Feb 2013; revised 12 Apr 2013; accepted 12 Apr 2013; published 17 Apr 2013

injection of 70 mA for the SOA section. The SOA was found to have a negligible influence on the laser performance.

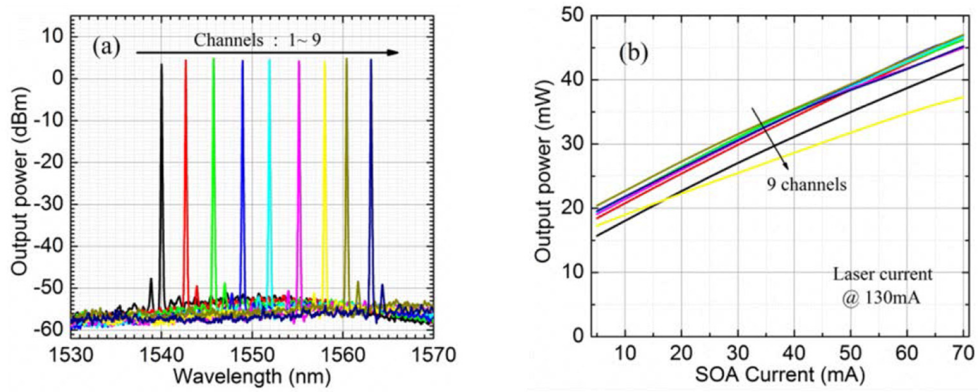

Fig. 4. Measured laser performance for the 9 channels with a total driving current of around 130 mA of each laser (a) output spectrum with SOA section unbiased; (b) output power vs. SOA current injection.

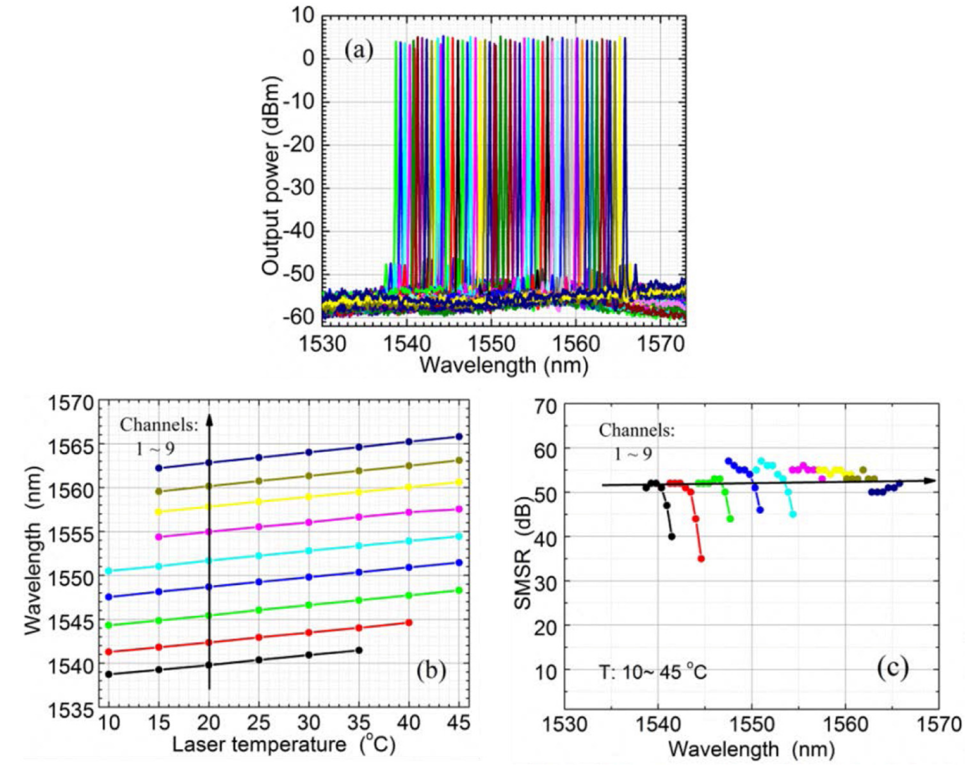

Fig. 5. Measured wavelength tuning behaviour of the fabricated laser array at the laser driving current of around 130 mA over the temperature range from 10˚C to 45˚C: (a) output spectrum; (b) Lasing wavelength vs. temperature; (c) SMSR vs. lasing wavelength.

We next check the wavelength tuning behavior of the fabricated laser array. We kept the total driving current of the laser section of around 130 mA and scanned the output spectrum by changing the chip temperature through the TEC. The currents were set the same as that in Fig. 4 (a) for each channel laser during this temperature tuning process. Figure 5(a) shows the

#186129 - $15.00 USD Received 28 Feb 2013; revised 12 Apr 2013; accepted 12 Apr 2013; published 17 Apr 2013

measured output spectra over a temperature range from 10˚C to 45˚C with a temperature step of 5 degree. Figure 5(b) plots the measured lasing wavelength versus the chip temperature for all the 9 channels within the laser array. It can be seen that a wavelength quasi-continuous tuning range of about 27 nm was obtained over the 35 degree temperature range. The measured SMSR of the laser array is plotted in Fig. 5(c) as a function of lasing wavelength during the temperature tuning, which shows the SMSR was more than 35dB over the whole tuning range. The drop of the SMSR from over 50 dB to above 35 dB for the channels on the short wavelength side with increased temperature is not caused by competition from the modes adjacent to the lasing mode but from the mode which is one free spectral range (FSR) longer, where the FSR is determined by the slot period to be about 40 nm. In our future work non-periodically spaced slots will be used to suppress these reflection peaks which are one FSR away from the main peak. This can be done by simply using a three-period structure as demonstrated in our previous work [15].

In summary, we present 9-channel wavelength tunable single mode laser array based on slots. The fabricated laser array exhibits a threshold current range of 19~21mA. The stable single mode performance is obtained for all the 9 channel lasers with side-mode suppression-ratio >50 dB at 20°C. The output power of the laser array reaches 37 mW with the total driving current of 130 mA of the laser section when the SOA is biased at 70 mA. By tuning the chip temperature a quasi-continuous tuning range ~27 nm is achieved over a temperature range from 10°C to 45°C. The presented laser array structure just needs a single wafer growth and can be fabricated by standard photolithography. It is also monolithically integrable to other devices. In addition, it can potentially achieve a high single mode yield. Therefore such a laser array platform has strong application potentials in optical communication systems.

Acknowledgment

This work is supported by science foundation of Ireland (SFI) under grant numbers 10/CE/I1853 and 12/TIDA/I2430.